

Endogenous Intracellular Calcium Buffering and the Activation/Inactivation of HVA Calcium Currents in Rat Dentate Gyrus Granule Cells

GEORG KÖHR and ISTVAN MODY

From the Department of Neurology and Neurological Sciences, Stanford University School of Medicine, Stanford, California 94305

ABSTRACT Granule cells acutely dissociated from the dentate gyrus of adult rat brains displayed a single class of high-threshold, voltage-activated (HVA) Ca^{2+} channels. The kinetics of whole-cell Ca^{2+} currents recorded with pipette solutions containing an intracellular ATP regenerating system but devoid of exogenous Ca^{2+} buffers, were fit best by Hodgkin-Huxley kinetics (m^2h), and were indistinguishable from those recorded with the nystatin perforated patch method. In the absence of exogenous Ca^{2+} buffers, inactivation of HVA Ca^{2+} channels was a predominantly Ca^{2+} -dependent process. The contribution of endogenous Ca^{2+} buffers to the kinetics of inactivation was investigated by comparing currents recorded from control cells to currents recorded from neurons that have lost a specific Ca^{2+} -binding protein, Calbindin- $\text{D}_{28\text{k}}$ (CaBP), after kindling-induced epilepsy. Kindled neurons devoid of CaBP showed faster rates of both activation and inactivation. Adding an exogenous Ca^{2+} chelator, 1,2-bis-(2-aminophenoxy)ethane- N,N,N',N' -tetraacetic acid (BAPTA), to the intracellular solution largely eliminated inactivation in both control and kindled neurons. The results are consistent with the hypothesis that endogenous intraneuronal CaBP contributes significantly to submembrane Ca^{2+} sequestration at a concentration range and time domain that regulate Ca^{2+} channel inactivation.

INTRODUCTION

The physiological consequences of calcium (Ca^{2+}) entry into neurons through voltage- or receptor-gated channels are distinct from ion flow through other ionic channels (Tsien, 1983). Whereas other channels serve merely as regulators of cellular electrical activity, an increase in the cytoplasmic free Ca^{2+} concentration ($[\text{Ca}^{2+}]_i$) has important second messenger-type effects on diverse neuronal functions by modulating Ca^{2+} -dependent cellular events (Swanson, 1989). In all cells there is a need to maintain resting $[\text{Ca}^{2+}]_i$ at levels below the threshold for activation of Ca^{2+} -dependent processes and to cope with the large Ca^{2+} entry during activity. Neurons, because of

Address reprint requests to Dr. Istvan Mody, Dept. of Neurology and Neurological Sciences, Stanford University School of Medicine, Rm. M016, Stanford, CA 94305.

their multitude of voltage- and receptor-operated ionic channels, are particularly prone to elevations in $[Ca^{2+}]_i$ and have a highly sophisticated protective machinery against excessive changes in intracellular Ca^{2+} activity. There are several intraneuronal systems including the mitochondria, endoplasmic reticulum, and cytosolic proteins to buffer the bulk of Ca^{2+} entry during activation of ionic channels (Carafoli, 1987; McBurney and Neering, 1987).

The rise of $[Ca^{2+}]_i$ also exerts an important low-gain negative feedback control over the entry of Ca^{2+} through voltage-dependent Ca^{2+} channels (Kostyuk and Krishtal, 1977; Tillotson, 1979; Brehm, Eckert, and Tillotson, 1980; Ashcroft and Stanfield, 1981; Eckert and Tillotson, 1981; Plant, Standen, and Ward, 1983; Plant, 1988). In neurons, the inactivation of some voltage-gated Ca^{2+} channels is both voltage and Ca^{2+} dependent (Brown, Morimoto, Tsuda, and Wilson, 1981; Eckert and Chad, 1984; Morad, Davies, Kaplan, and Lux, 1988; Gutnick, Lux, Swandulla, and Zucker, 1989; Schroeder, Fischbach, Mamo, and McCleskey, 1990; Yue, Backx, and Imredy, 1990). The molecular mechanisms of the Ca^{2+} -dependent inactivation process are not well understood, but it is clear that the Ca^{2+} -dependent inactivation depends on the effectiveness of submembrane intracellular Ca^{2+} -buffering systems which may rapidly sequester Ca^{2+} before reaching the site of control for inactivation (Eckert and Chad, 1984). To date, in whole-cell recordings of Ca^{2+} currents in mammalian neurons, the endogenous intracellular Ca^{2+} buffering mechanism may have been overlooked by the intracellular addition of exogenous Ca^{2+} chelators such as EGTA or BAPTA via conventional patch pipettes. To address this issue, in the experiments reported here, Ca^{2+} currents were mainly evoked in the absence of an exogenous Ca^{2+} chelator, similar to the approach of Kalman, O'Laigue, Erxleben, and Armstrong (1988) in pituitary tumor cells (GH₃).

One component of the endogenous intraneuronal Ca^{2+} -buffering mechanism consists of high-affinity Ca^{2+} -binding proteins such as calmodulin (CaM), parvalbumin (PV), calretinin, and calbindin-D_{28k} (CaBP). These proteins are ideally suited to sequester the excess Ca^{2+} that accumulates at the site of Ca^{2+} entry. This function has been postulated for CaBP (Baimbridge and Miller, 1982; Celio, 1990; Mody, Reynolds, Salter, Carlen, and MacDonald, 1990) and consequently the lack of cytoplasmic CaBP found in certain neurons may result in their selective Ca^{2+} -dependent vulnerability. Recent findings of reduced CaBP levels in degenerating neurons with a subsequent impairment of their intracellular Ca^{2+} regulation support this hypothesis (McLachlan, Wong, Bergeron, and Baimbridge, 1987; Ichimiya, Emson, Mountjoy, Lawson, and Heizmann, 1988; Seto-Ohshima, Lawson, Emson, Mountjoy, and Carrasco, 1988; Scharfman and Schwartzkroin, 1989; Sloviter, 1989; Mattson, Rychlik, Chu, and Christakos, 1991).

To study the contribution of the protein component to the endogenous neuronal Ca^{2+} buffering mechanisms we have compared the activation and inactivation of high-threshold, voltage-activated (HVA) Ca^{2+} currents in granule cells of the control dentate gyrus recorded with or without exogenous Ca^{2+} chelators to a granule cell preparation with specifically lower levels of neuronal CaBP after kindling-induced epilepsy (Baimbridge and Miller, 1982; Köhr, Lambert, and Mody, 1991). The observed differential Ca^{2+} -dependent inactivation of HVA Ca^{2+} channels in control and kindled neurons strongly supports the hypothesis that CaBP contributes to the

submembrane Ca²⁺ buffering. Thus, through the removal of Ca²⁺, CaBP can affect Ca²⁺-dependent cellular events including the inactivation of Ca²⁺ channels.

Preliminary findings of this report have been published as an abstract (Köhr, Lambert, and Mody, 1990).

METHODS

Dissociation of Neurons

Coronal half-brain slices, 400 μ m thick, were prepared on a Lancer Vibratome (series 1000; Technical Products International Inc., St. Louis, MO) in ice-cold artificial cerebro-spinal fluid (a.c.s.f.) after the dissection of the brain from Na-pentobarbital (65 mg/kg i.p.) anesthetized male Wistar control or kindled rats (300–600 g). The slices were maintained in a storage chamber for at least 1 h at 32°C containing a.c.s.f. with the following composition (in mM): 126 NaCl, 2.5 KCl, 2 MgCl₂, 2 CaCl₂, 1.25 NaH₂PO₄, 10 glucose, 26 NaHCO₃, and 1 pyruvic acid, pH 7.35. The a.c.s.f. was constantly gassed with a warmed (32°C) and humidified O₂/CO₂ gas mixture (95/5%). Before microdissecting the dentate gyrus, a single slice was incubated for 30 min (32°C) in 3 ml oxygenated a.c.s.f. with 1.5 mg/ml pronase (protease type XIV; Sigma Chemical Co., St. Louis, MO) for enzymatic digestion (Mody, Salter, and MacDonald, 1989). The dentate gyrus was triturated using a fire-polished Pasteur pipette in a test tube containing 3 ml cold *N*-2-hydroxyethylpiperazine-*N'*-2-ethanesulfonic acid (HEPES)-buffered a.c.s.f. (the NaHCO₃ was replaced by equimolar HEPES). The neuronal suspension was then transferred into a tissue culture dish (Lux, 35 mm; Nunc, Inc., Naperville, IL). After the neurons settled down in the dish (~3–5 min) they were washed at least two times with the recording solution.

Extracellular Recording Solution

Ca²⁺ currents were recorded in the following extracellular solution (in mM): 106 NaCl, 2.5 KCl, 2 MgCl₂, 5 CaCl₂, 3 CsCl, 25 tetraethylammonium chloride (TEA), 5 4-aminopyridine, 1 pyruvic acid, 10 glucose, and 20 HEPES. The pH was adjusted to 7.25 with CsOH; after adding 1 μ M tetrodotoxin (TTX) the final solution had an osmolarity of 290–300 mosM. Usually, the recording solution was not changed during recording periods up to 2 h in the same dish at room temperature (21–23°C). To test the sensitivity of the Ca²⁺ currents to cadmium the contents of the dish were exchanged with a 200 μ M Cd²⁺-containing extracellular medium during the recording.

Perforated Patch Recordings

The pipette solution contained (in mM): 100 Cs₂SO₄, 20 CsCl, 8 MgCl₂, and 10 HEPES (pH 7.35, 290 mosM). Nystatin (300–600 μ g/ml; Sigma Chemical Co. or Squibb) was added from a stock solution (50 mg/ml) in dimethyl sulfoxide (DMSO). This solution was briefly vortexed and sonicated in a water bath for 30 s (Horn and Marty, 1988). Despite filling the tip of the electrode with a relatively high concentration of nystatin solution, it took at best 20–50 min for the membrane to perforate and the series resistance to drop to <30 M Ω .

Solutions for Intracellular Dialysis

Intracellular solutions contained (in mM): 110 CsCl, 3 TEA, 10 HEPES, and an ATP regenerating system (4 mM Mg-ATP, 25 mM phosphocreatine, and 50 U \times ml⁻¹ creatine-phosphokinase; Forscher and Oxford, 1985) for half of the experiments (Ca²⁺ chelator-free recordings). The pH was adjusted to 7.25 (265–285 mosM). For the other half of the experiments the Ca²⁺-buffering system consisted of 5 mM 1,2-bis-(2-aminophenoxy)ethane-

N,N,N',N'-tetraacetic acid tetrapotassium salt (BAPTA; Sigma Chemical Co.) and 0.5 mM CaCl_2 (pH 7.25; 270–290 mosM). To avoid a loss in efficacy of the ATP regenerating system, the solutions were used freshly or aliquotted into smaller batches and frozen at -80°C until use. Solutions older than 1 wk were discarded. To compensate for a possible Ca contamination of the intracellular solution (originating from glassware or contaminated chemicals), 5 μM BAPTA was added to the Ca^{2+} chelator-free recordings in some of the experiments. Under such recording conditions inactivation of Ca^{2+} currents was comparable to recordings done in the total absence of BAPTA.

Electrodes and Whole-Cell Recordings

Patch electrodes were pulled from borosilicate thin-walled glass (o.d. 1.5 mm, i.d. 1.12 mm with filament; Garner Glass Co., Claremont, CA) on a Narishige PP-83 two-stage vertical puller (Narishige Scientific Laboratory, Tokyo, Japan). Once filled, electrodes had resistances of 4–7 M Ω . We did not find it necessary to fire-polish or coat the electrodes.

After gigaseal (>3 G Ω) formation, whole-cell voltage-clamp recordings (Hamill, Marty, Neher, Sakmann, and Sigworth, 1981; Marty and Neher, 1983) of Ca^{2+} currents were evoked from various holding potentials and amplified by a List EPC-7 amplifier (filtered at 3 kHz, 3-pole Bessel filter, -3 dB; List-Medical-Electronic, Darmstadt, Germany). The series resistance was compensated by $>75\%$. Command voltage steps were generated using the VGEN program of the Strathclyde Electrophysiology Software through a DT 2801 or DT 2821 D/A converter of an IBM-AT compatible computer. All recordings were done at room temperature (21 – 23°C) and were stored on videotapes after pulse-code modulation by a Neurocorder DR-484 (Neuro Data Instruments Corp., New York, NY; digitization rate, 44 kHz).

Data Analysis and Curve Fitting

The data were analyzed off-line by digitizing at 12.5 kHz using the VCAN and SCAN programs of the Strathclyde Electrophysiology Software (courtesy of J. Dempster, Dept. of Physiology and Pharmacology, University of Strathclyde, Glasgow, UK). Statistical analysis included the one-way ANOVA test and the two-tailed Mann-Whitney U-test (e.g., Zar, 1984). All results are expressed as mean \pm SD.

The time course of activation and inactivation of I_{Ca} during 100-ms depolarizations were fitted with Hodgkin-Huxley (m^2h) kinetics of the form:

$$I(t) = I_{\text{max}} [1 - \exp(-t/\tau_m)]^2 \times [h_{\text{inf}} - (h_{\text{inf}} - 1) \exp(-t/\tau_h)]$$

where $I(t)$ is the activating/inactivating current as a function of time, I_{max} is the maximum current amplitude, τ_m is the time constant of the activation parameter, τ_h is the time constant, and h_{inf} is the steady-state value of the inactivation parameter.

The time course of I_{Ca} inactivation during 1,000-ms depolarizations were fitted with the double-exponential function:

$$y(t) = A \times \exp(-t/\tau_{\text{fast}}) + B \times \exp(-t/\tau_{\text{slow}}) + C$$

where $y(t)$ is the inactivating current as a function of time, A and B are the best-fitting amplitudes, τ_{fast} and τ_{slow} are the best-fitting time constants for the two exponential decays, and C is the steady-state value. Hodgkin-Huxley and double-exponential fits were performed using a Levenberg-Marquardt algorithm.

The steady-state inactivation was fitted by the following Boltzmann equation:

$$I/I_{\text{max}} = \{1 + \exp[(V - V_{1/2})/k]\}^{-1}$$

where I_{max} is the maximum current amplitude, $V_{1/2}$ is the half-inactivating voltage, and k is a constant. A Simplex algorithm was used to perform the fits.

Kindling

Stainless steel bipolar stimulating electrodes were implanted in the midline hippocampal commissural pathway of male Wistar rats (190–210 g) under Na-pentobarbital anesthesia (65 mg/kg i.p.). The coordinates for electrode positions were 1.8 mm posterior to bregma, midline, and 4.2 mm below the surface of the cortex. After at least 1 wk of postsurgical recovery the rats received daily stimulations (1-s, 60-Hz stimulus train of 100–150 μ A) and the afterdischarges and poststimulus behavior were observed. All kindled rats used in this study fulfilled the criterion for full kindling (i.e., at least five consecutive stage 5 motor seizures; Racine, 1972) and had 10–20 seizures at the day of sacrifice (24–72 h after the last stimulation). Control rats consisted of both implanted but not stimulated animals and unimplanted, age-matched animals.

RESULTS

Ca^{2+} Currents Recorded in the Whole-Cell Configuration with an ATP Regenerating System and Using the Perforated Patch Technique

Ca^{2+} currents (I_{Ca}) could be evoked in isolation by adding TTX to block sodium currents, while potassium currents were minimized by the combination of external 4-aminopyridine and TEA and internal CsCl and TEA. Under these conditions, prominent I_{Ca} were recorded in an external solution containing 5 mM Ca^{2+} .

Fig. 1 shows leak-subtracted I_{Ca} and I - V relationships in dentate gyrus granule cells dissociated from control rats using the ATP regenerating system in the absence of the Ca^{2+} chelator BAPTA (Fig. 1 *A*) and using the perforated patch technique (Fig. 1 *B*). I_{Ca} were evoked from a holding potential (V_h) of -50 mV. The I_{Ca} showed similar kinetics in both recording techniques applied. The threshold for activation of I_{Ca} was between -40 and -30 mV and the maximal I_{Ca} was evoked by command potentials to $+10$ mV. With progressively stronger depolarizing pulses (up to $+80$ mV) the currents became smaller and reversed between $+50$ and $+70$ mV. The net outward current may be due to a Cs^+ efflux larger than Ca^{2+} entry through Ca^{2+} channels at these depolarized potentials (Fenwick, Marty, and Neher, 1982). Because of the inefficiency of the perforated patch recording technique in these neurons ($n = 4$; see Methods) and the comparable results obtained in whole-cell recordings, I_{Ca} were studied exclusively in the whole-cell configuration using the ATP regenerating solution.

Ca^{2+} Current Recordings with No Exogenous Ca^{2+} Chelator in Granule Cells Dissociated from Control and Kindled Rats

To test the endogenous Ca^{2+} sequestering capacity in control and kindled granule cells, I_{Ca} were recorded in the absence of an exogenous Ca^{2+} chelator. Fig. 2 (open symbols) shows I - V relationships of leak-subtracted I_{Ca} in a control (Fig. 2 *A*) and a kindled (Fig. 2 *B*) neuron. Maximal I_{Ca} were evoked by command potentials to $+10$ mV from a V_h of -50 mV. The average maximal amplitude was 269.3 ± 72.3 pA

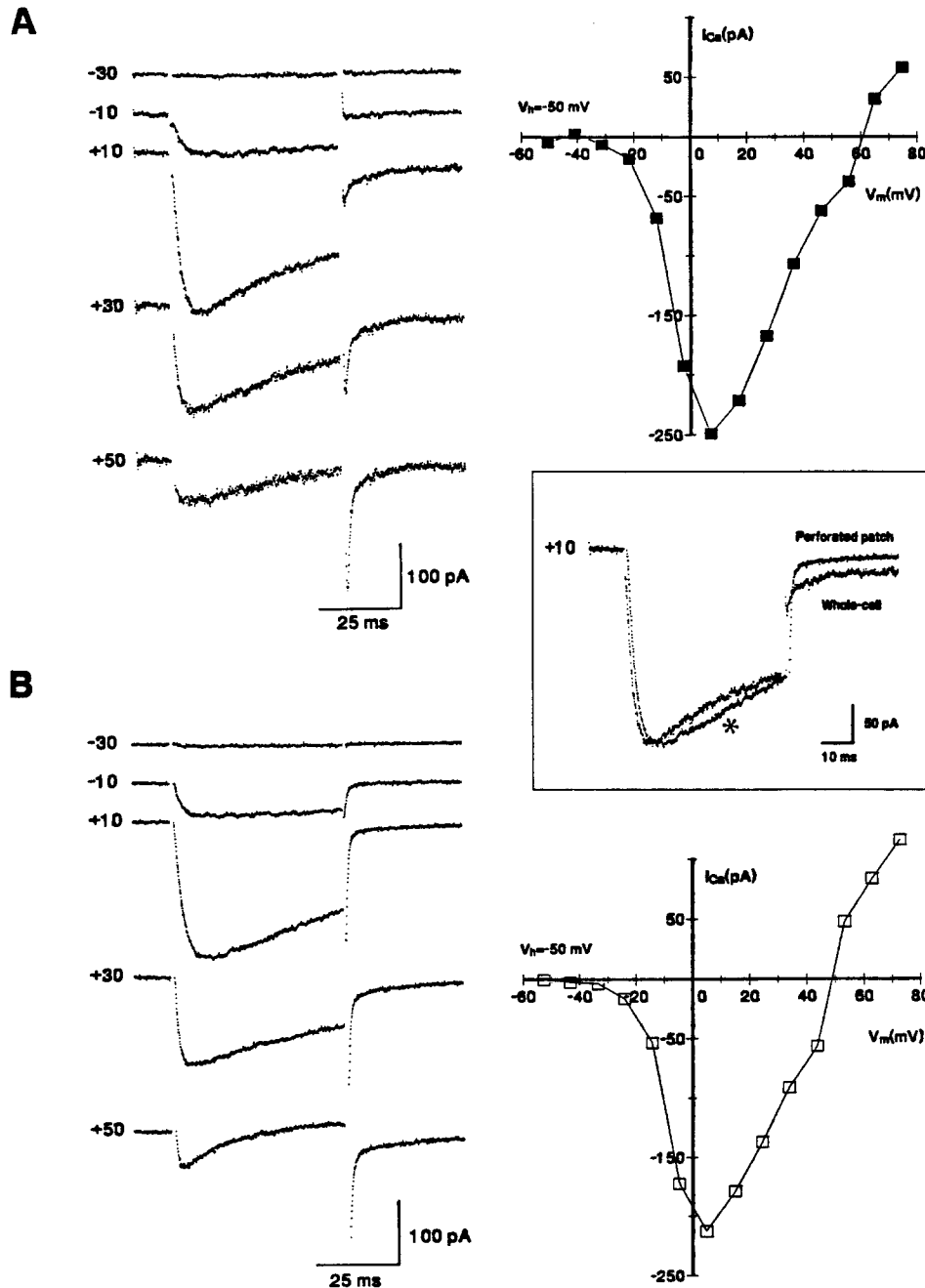


FIGURE 1. Leak-subtracted Ca^{2+} currents (I_{Ca}) and corresponding I - V plots recorded 15–25 min after establishing whole-cell configuration with an ATP regenerating system in the absence of an exogenous Ca^{2+} chelator (*A*), and using the perforated patch technique (*B*) in acutely isolated granule cells. Note the similar amplitudes, shapes, and voltage dependencies of I_{Ca} in both recording techniques. At +10 mV, I_{Ca} inactivated at the end of the 50-ms depolarizing

($n = 12$) in control granule cells and 265.4 ± 106.7 pA ($n = 13$) in kindled granule cells.

At a V_h of -50 mV there was no indication of a second type of I_{Ca} in the I - V relationship. At holding potentials as negative as -100 mV there was only a negligible contribution of other, low voltage-activated (LVA) I_{Ca} (Carbone and Lux, 1984; Fox, Nowycky, and Tsien, 1987) to the prominent HVA I_{Ca} (Carbone and Lux, 1984; Fox et al., 1987) (Fig. 2, *A* and *B*, filled symbols). No LVA I_{Ca} could be evoked by command potentials up to -20 mV in either control (Fig. 2 *A*) or kindled (Fig. 2 *B*) neurons. It appears that only one type of Ca^{2+} channel dominates in the adult dentate gyrus granule cells as demonstrated in a recent study (Fisher, Gray, and Johnston, 1990). The HVA I_{Ca} in both control and kindled neurons were completely abolished by perfusion of cadmium ($200 \mu\text{M}$) (Fig. 2 *C*).

Two differences between I_{Ca} recorded from control and kindled granule cells became obvious after superimposing leak-unsubtracted I_{Ca} during 50-ms depolarizing commands (Fig. 2 *D*). First, in the absence of an exogenous Ca^{2+} chelator, at the end of a 50-ms command voltage pulse peak, I_{Ca} in kindled granule cells were more inactivated than I_{Ca} recorded from control granule cells. Second, I_{Ca} activation appeared to be faster in kindled neurons.

Activation and Inactivation Rates in Control and Kindled Neurons

To study the activation and inactivation kinetics of I_{Ca} in the absence of an exogenous Ca^{2+} chelator, we applied depolarizing commands of 100 ms duration in control and kindled neurons from a holding potential of -50 mV (Fig. 3). Hodgkin-Huxley kinetics (m^2h) were fitted to the I_{Ca} and are shown as smooth curves on top of each scatter plot.

The fits during the first 30 ms of depolarization are superimposed in Fig. 4 *A*. For all potentials tested the activation rate ($1/\tau_m$) of I_{Ca} was faster in kindled ($n = 5$) than in control neurons ($n = 6$; Fig. 4 *B*). With increasing membrane potentials (-10 to $+30$ mV) the activation rate of control I_{Ca} increased from 371.7 ± 57.4 to 723.0 ± 87.3 s^{-1} ($n = 6$), while the activation rate of kindled I_{Ca} increased from 551.6 ± 50.2 to 832.5 ± 98.5 s^{-1} ($n = 5$). Analysis of the inactivation rate ($1/\tau_h$) in the same neurons showed faster kinetics in kindled neurons (Fig. 4 *C*). With increasing membrane potentials the inactivation rate increased and was maximal at 10 mV, where the largest I_{Ca} were elicited. At $+10$ mV the inactivation rate was 18.8 ± 3.3 s^{-1} ($n = 6$) in control neurons and 29.9 ± 2.2 s^{-1} ($n = 5$) in kindled neurons. With further depolarizations (up to $+30$ mV) the inactivation rate decreased and thus became U-shaped for the whole potential range analyzed.

pulse by 42% in *A* and by 38% in *B*. Holding potential was -50 mV and the extracellular Ca^{2+} concentration was 5 mM. The inset shows superimposed Ca^{2+} currents evoked by a command potential to $+10$ mV recorded with the whole-cell and the perforated patch method (marked by *). Note the similarity in the kinetics regardless of the recording method used, indicating that the whole-cell recording with no added exogenous Ca^{2+} chelators mimics the unperturbed intracellular environment of dentate gyrus granule cells. The nystatin trace has been multiplied by 1.19 to match the peak of the whole-cell current.

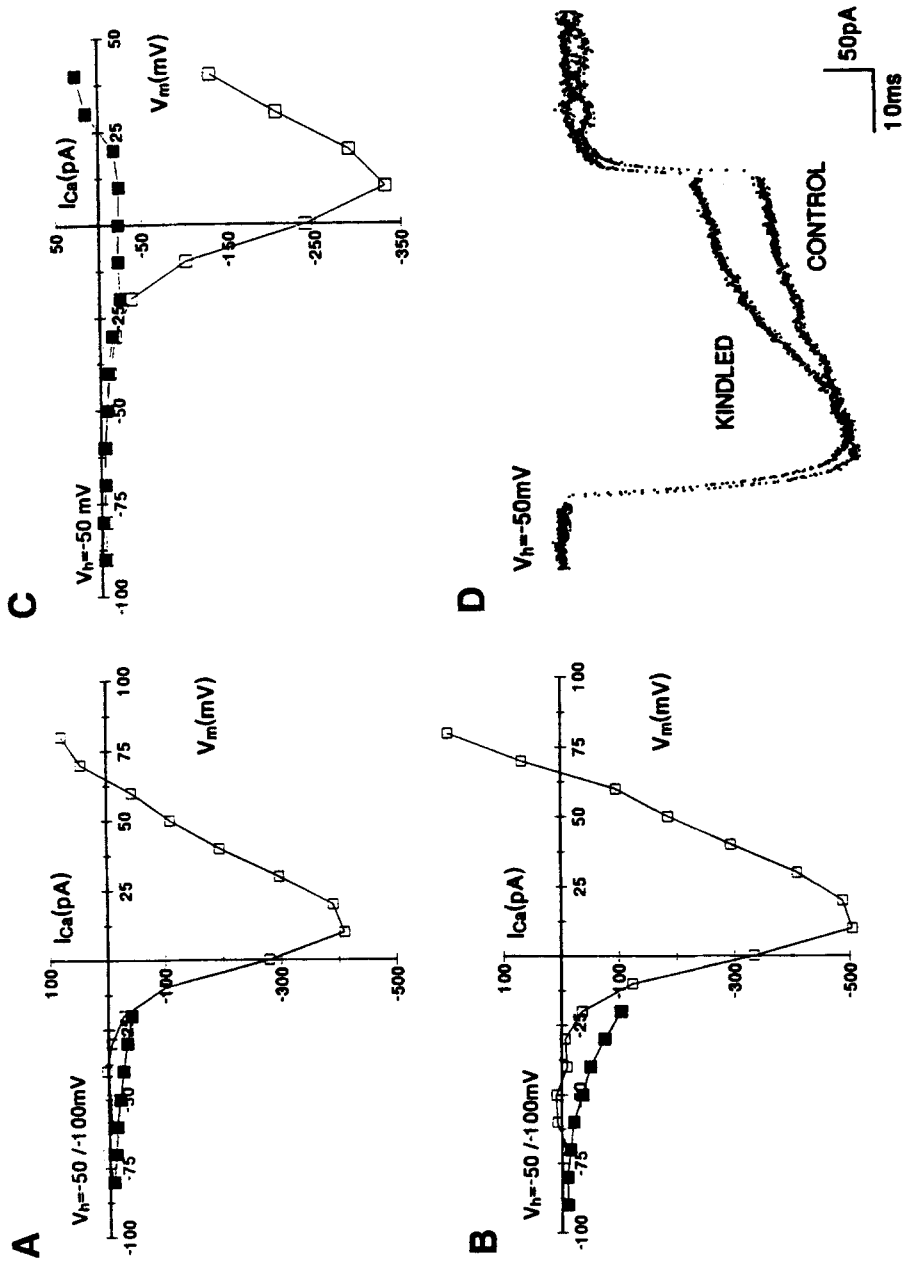


FIGURE 2

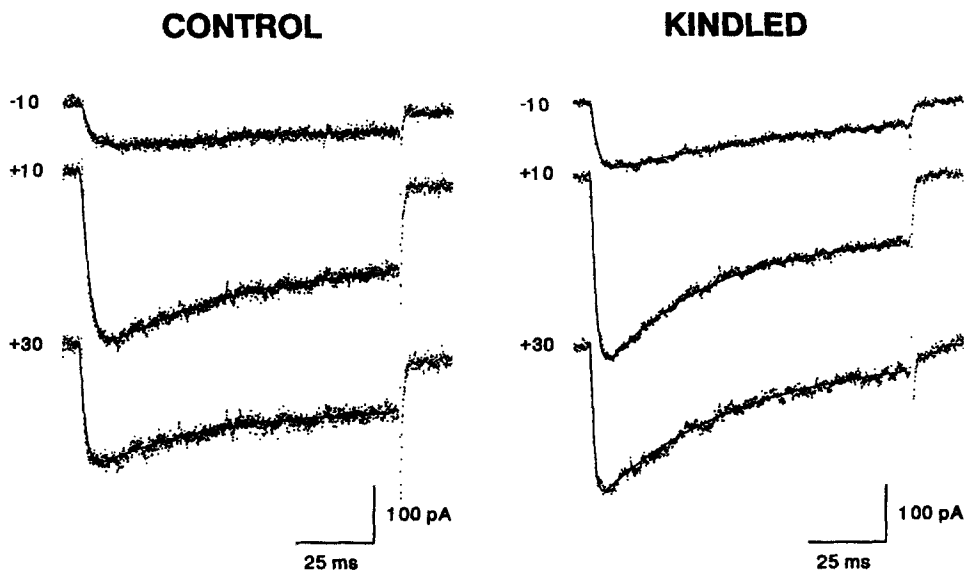


FIGURE 3. Hodgkin-Huxley kinetics are shown as smooth curves for leak-subtracted I_{Ca} evoked from -50 mV to potentials indicated in a control and a kindled granule cell in the absence of an exogenous Ca^{2+} chelator. Note the faster decay of I_{Ca} in the kindled granule cell during 100-ms depolarizations. For further details see Fig. 4.

Exogenous Ca^{2+} Chelators

The enhanced activation and inactivation rates of I_{Ca} after kindling might result from the loss of the intraneuronal Ca^{2+} -binding protein CaBP, as illustrated by immunohistochemistry (Miller and Baimbridge, 1983; Köhr et al., 1991). Therefore, intracellular dialysis (Marty and Neher, 1983) of an exogenous Ca^{2+} chelator should change the time course of I_{Ca} activation and inactivation at least in kindled granule cells. We used BAPTA as an exogenous Ca^{2+} chelator to study its effect on I_{Ca} inactivation, because BAPTA is approximately five times more efficient and faster in chelating Ca^{2+} ions than EGTA (Tsien, 1980; Marty and Neher, 1983) and doesn't allow a marked I_{Ca} inactivation (Kalman et al., 1988; Plant, 1988). Intracellular dialysis of 5 mM BAPTA/0.5 mM $CaCl_2$ ($[Ca^{2+}]_i = 2 \times 10^{-8}$ M) did not change the peak I_{Ca} . This was tested by two subsequent recordings ($n = 4$) in the same neuron: first with no BAPTA in the electrode and then with a BAPTA containing fill in a second patch electrode. After withdrawal of the first electrode from the cell, the second seal was

FIGURE 2. (*opposite*) I - V relationships for I_{Ca} recorded in granule cells dissociated from a control (*A*) and a kindled (*B*) rat in the absence of BAPTA. Depolarizing pulses (50 ms) from holding potentials (V_h) of -50 mV (\square) evoked a HVA I_{Ca} . Preceding hyperpolarizations (1 s) to -100 mV (\blacksquare) increased the amplitude of the HVA current but failed to uncover a LVA I_{Ca} . Perfusion of 200 μ M cadmium (\blacksquare) blocked the HVA in control (*C*) and kindled (not shown) granule cells. (*D*) increased inactivation of I_{Ca} during a 50-ms depolarizing pulse to $+10$ mV in kindled granule cells in the absence of an exogenous Ca^{2+} chelator. The capacitive transients of the leak-unsubtracted current traces are blanked out.

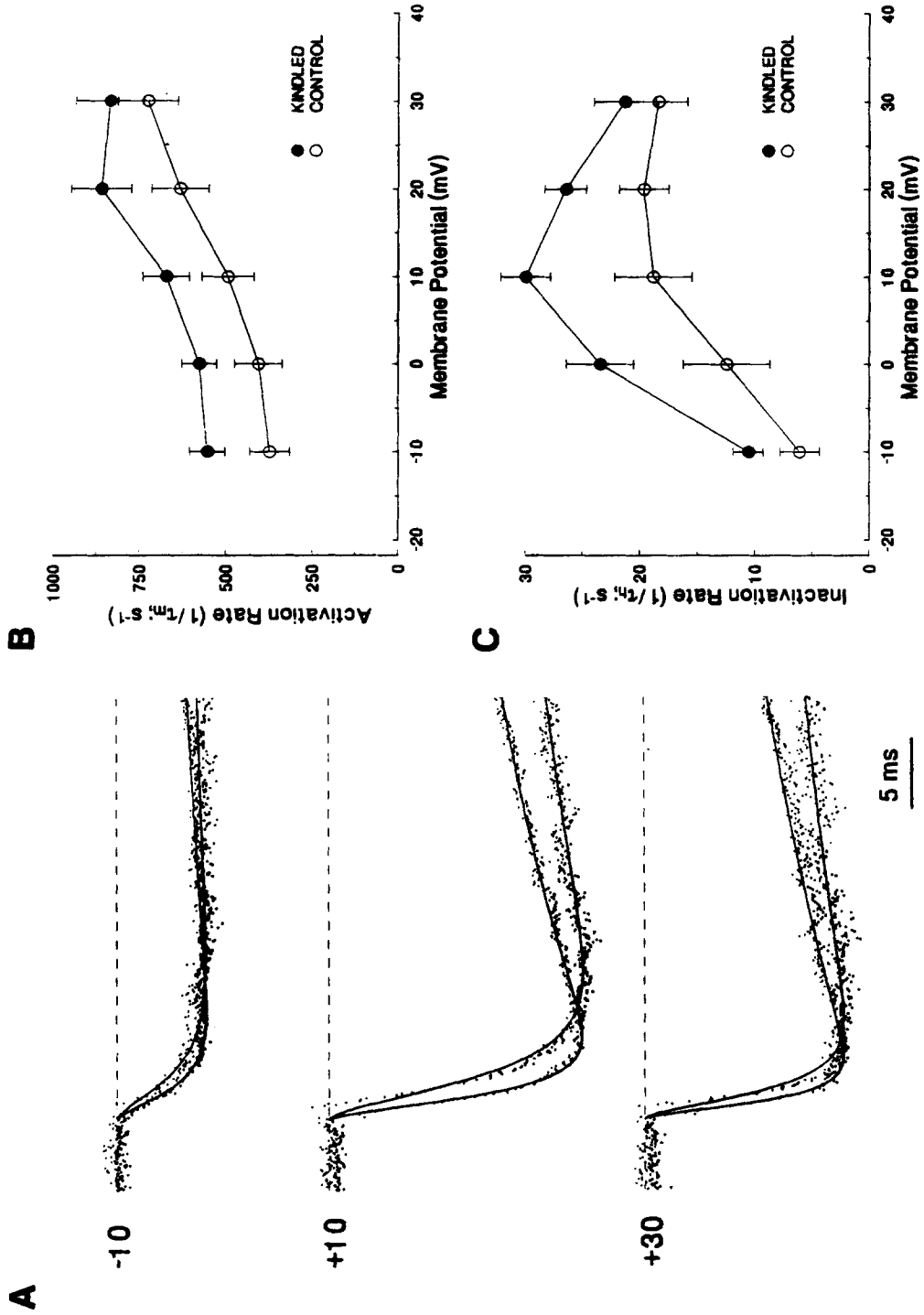


FIGURE 4

TABLE I
Comparison of the Average Peak Ca²⁺ Currents (I_{peak}) Recorded in Control and Kindled Neurons with and without Intracellular BAPTA

	<i>n</i>	<i>I_{peak}</i> (mean ± SD)	<i>I_{peak}/I_{50 ms}</i> (mean ± SD)
		<i>pA</i>	%
Control	12	269.3 ± 72.3	30.6 ± 8.2 ^a
Kindled	13	265.4 ± 106.7	52.4 ± 8.2 ^b
Control + BAPTA	11	285.6 ± 124.1	4.6 ± 3.5 ^c
Kindled + BAPTA	9	324.9 ± 112.8	5.6 ± 2.8 ^c

At the end of a 50-ms depolarizing pulse *I_{peak}* decayed significantly faster in kindled neurons than in controls (see also inactivation curves in Figs. 5 and 6). After BAPTA-loading *I_{peak}* decayed slower in both control and kindled neurons, but the decays in the two groups were not different from each other. Different superscript lowercase letters indicate significant differences ($P < 0.001$, ANOVA) between compared groups. The *I_{peak}* was not significantly different in any of the groups.

usually less successful than the first, producing a faster deterioration of the second recording. For this reason, most recordings using BAPTA were done without a preceding BAPTA-free recording.

The amplitude of *I_{Ca}* in the presence of intracellular BAPTA was 285.6 ± 124.1 pA ($n = 11$) in control granule cells and 324.9 ± 112.8 pA ($n = 9$) in kindled neurons, moderately increased compared with BAPTA-free recordings (Table I). At the end of a 50-ms command voltage pulse to +10 mV the *I_{Ca}* were inactivated by only ~5% in control and kindled neurons. The activation rate was accelerated in both control and kindled neurons after BAPTA loading. At +10 mV the rate of activation was 631.8 ± 65.2 s⁻¹ ($n = 4$) in control granule cells and 724.0 ± 49.2 s⁻¹ ($n = 4$) in kindled granule cells (values for BAPTA-free situation: control, 491.7 ± 74.5 s⁻¹ ($n = 5$); kindled granule cells, 669.8 ± 66.4 s⁻¹ ($n = 6$)).

Double-Pulse Experiments: Effects of Prior Ca²⁺ Entry on Test Ca²⁺ Currents

Inactivation of *I_{Ca}* involves a Ca²⁺-dependent process which can be demonstrated by the inactivation of the current after prior Ca²⁺ entry in double-pulse experiments (for review, see Eckert and Chad, 1984). The command voltage during a 50-ms conditioning pulse (*P*₁) was systematically varied and the effect on peak *I_{Ca}* during a subsequent test pulse (*P*₂), evoked 50 ms later by a step to +10 mV, was measured (see Fig. 5, *inset*). The *V_h* was -50 mV throughout the experiment. Ca²⁺ currents evoked during the conditioning pulses (*I_{Ca}*(*P*₁)) are shown normalized to peak current for 12 control

FIGURE 4. (*opposite*) (A) The Hodgkin-Huxley fits of Fig. 3 are shown superimposed for the first 30 ms. For each step potential the faster activating and faster inactivating *I_{Ca}* originate from the kindled granule cell. (B) The activation rate of *I_{Ca}* is plotted as a function of membrane potential and is larger for the kindled granule cell at all potentials analyzed. (C) The inactivation rate plotted as a function of membrane potential is faster in kindled neurons and maximal at +10 mV, which activates the largest *I_{Ca}*. In this and all subsequent figures error bars represent standard deviation.

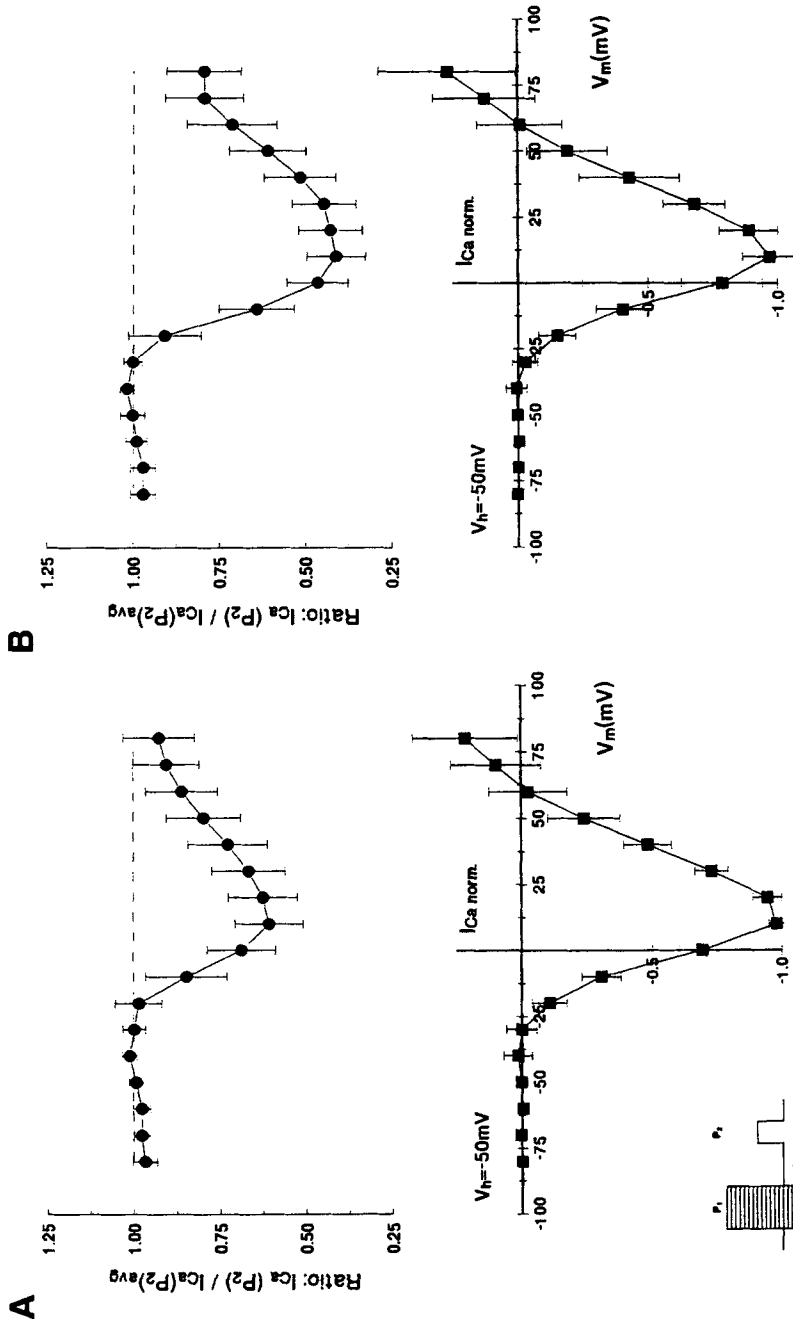


FIGURE 5. Inactivation of I_{Ca} plotted as a function of the conditioning membrane potential in double-pulse experiments. *A* illustrates the average of 12 control and *B* the average of 13 kindled granule cells. Conditioning pulses (P_1 , 50 ms) to different depolarizing membrane potentials were followed by test pulses (P_2 , 25 ms) to +10 mV after 50 ms of repolarization to -50 mV (*inset*). I_{Ca} evoked during P_1 are shown after leak subtraction as normalized $I-V$ relationships. Four test currents evoked without conditioning I_{Ca} were normalized and averaged [$=I_{Ca}(P_2)_{avg}$]. The ratio between normalized test currents [$=I_{Ca}(P_2)$] evoked after conditioning Ca^{2+} currents and $I_{Ca}(P_2)_{avg}$ is plotted as a function of the conditioning membrane potential during P_1 . The inactivation curves are both U-shaped but the inactivation is significantly ($P < 0.001$, ANOVA) larger in kindled granule cells.

FIGURE 5. Inactivation of I_{Ca} plotted as a function of the conditioning membrane potential in double-pulse experiments. *A* illustrates the average of 12 control and *B* the average of 13 kindled granule cells. Conditioning pulses (P_1 , 50 ms) to different depolarizing membrane potentials were followed by test pulses (P_2 , 25 ms) to +10 mV after 50 ms of repolarization to -50 mV (*inset*). I_{Ca} evoked during P_1 are shown after leak subtraction as normalized $I-V$ relationships. Four test

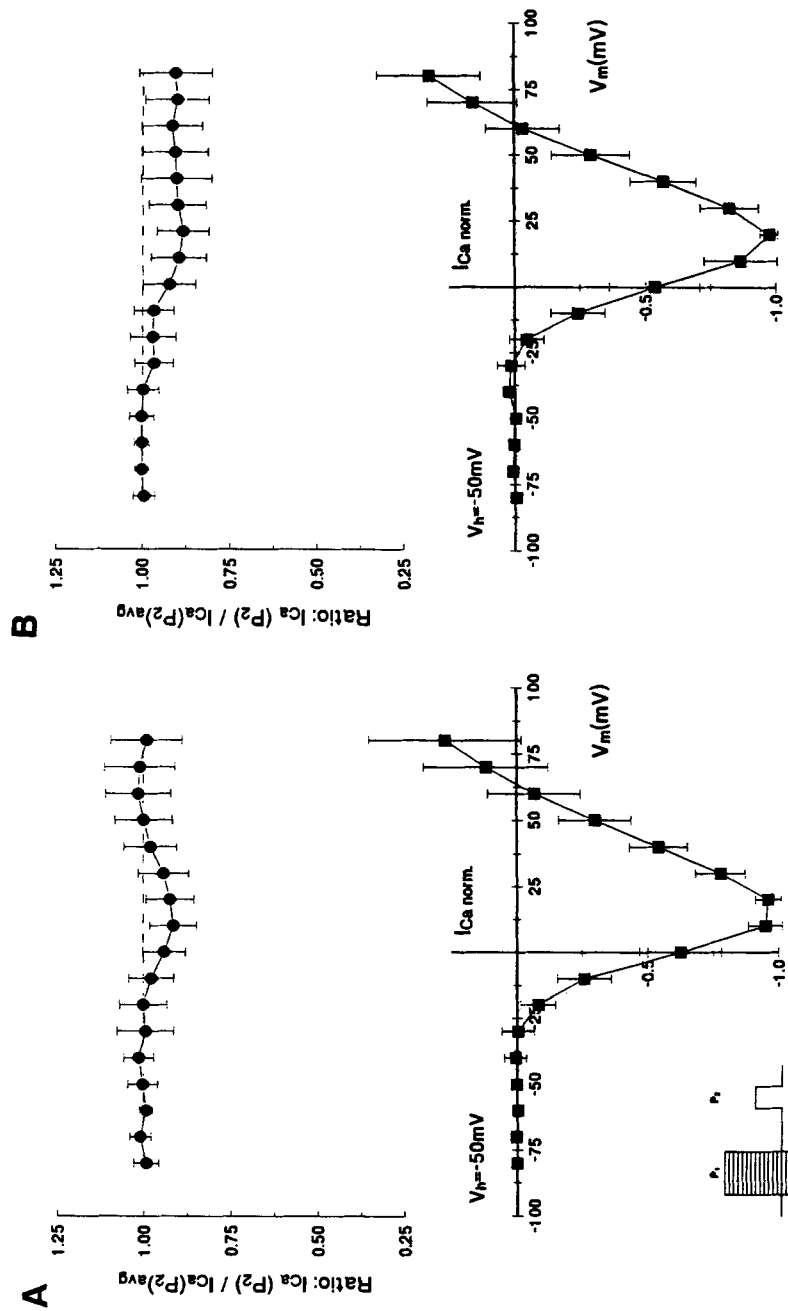


FIGURE 6. The same plots as in Fig. 5 averaged for 11 control (A) and 9 kindled (B) granule cells loaded with 5 mM BAPTA/0.5 mM $CaCl_2$. The inactivation is markedly reduced but not altogether prevented in both groups of neurons (see text for details). Note that the peak Ca^{2+} currents in the $I-V$ curves are now evoked with more depolarized membrane potentials (+20 mV).

(Fig. 5 *A*) and 13 kindled (Fig. 5 *B*) neurons. The corresponding absolute leak-subtracted maximal I_{Ca} are listed in Table I. The inactivation of the test $I_{Ca}(P_2)$ as a function of the P_1 potential is shown above the I - V relationships. In control granule cells (Fig. 5 *A*) inactivation increased with increasing I_{Ca} . It was largest ($39.3 \pm 9.9\%$, $n = 12$) at membrane potentials where the largest I_{Ca} were evoked and decreased at more positive potentials as the membrane potential approached the equilibrium potential for Ca^{2+} and Ca^{2+} entry was diminished. Such U-shaped inactivation curve reflects the dependence of I_{Ca} inactivation on Ca^{2+} entry during P_1 rather than on membrane voltage (for review, see Eckert and Chad, 1984). In kindled granule cells (Fig. 5 *B*) maximal I_{Ca} inactivation was significantly ($P < 0.001$, ANOVA) enlarged over control granule cells ($58.7 \pm 8.4\%$, $n = 13$) and occurred even in the presence of reduced Ca^{2+} entry at very high levels of depolarizations. Nevertheless, the inactivation curve was still U-shaped.

Loading control and kindled neurons with 5 mM BAPTA/0.5 mM $CaCl_2$ decreased the Ca^{2+} -dependent inactivation of I_{Ca} significantly ($P < 0.001$, ANOVA) in both groups of neurons (Fig. 6). The I_{Ca} inactivation was reduced in control granule cells to $8.7 \pm 6.7\%$ (Fig. 6 *A*; $n = 11$) and in kindled granule cells to $11.6 \pm 7.4\%$ (Fig. 6 *B*; $n = 9$). The two groups were now undistinguishable from each other. The remaining inactivation could be due to an insufficient BAPTA concentration or a weak voltage-dependent component of the I_{Ca} inactivation process.

Dependence of Inactivation on Ca^{2+} Entry

To further demonstrate the dependence of I_{Ca} inactivation on the amount of Ca^{2+} entering the cell, the duration of the conditioning pulse (P_1) was varied to yield different Ca^{2+} entries during P_1 . In all experiments, the interpulse interval was 50 ms. Fig. 7 shows the largest inactivation of test I_{Ca} caused by the maximal I_{Ca} evoked during 20-, 50-, or 100-ms conditioning pulses in control and kindled neurons. During 20-ms conditioning pulses the maximal I_{Ca} inactivation was similar in both groups of neurons: $33.6 \pm 15.4\%$ ($n = 5$) in control and $34.6 \pm 10.9\%$ ($n = 7$) in kindled granule cells. Extending the P_1 duration to 50 ms increased inactivation, especially in kindled neurons (see double-pulse experiments in Fig. 5). Extending P_1 to 100 ms resulted in a further increase of I_{Ca} inactivation to $51.2 \pm 5.1\%$ in control ($n = 3$) and $68.0 \pm 5.1\%$ in kindled ($n = 6$) neurons. It is interesting to note that the differences between the I_{Ca} inactivation of the control and kindled preparations became evident only after a threshold Ca^{2+} entry had been surpassed. This is consistent with the hypothesis that Ca^{2+} sequestering systems have a threshold and are more effective at higher cellular Ca^{2+} loading (Thayer and Miller, 1990).

We have integrated the leak-subtracted prepulse currents $I_{Ca}(P_1)$ in control ($n = 15$) and kindled ($n = 18$) neurons. As expected, the amount of charge entering the cell increased with longer pulse durations (20, 50, and 100 ms) but also with increasing peak current amplitudes within the same group. In Fig. 8 *A*, the charge carried by Ca^{2+} (picocoulomb) in two subsequent double-pulse experiments (50- and 100-ms P_1 duration) are illustrated for one control and one kindled granule cell. A minimum Ca^{2+} influx during P_1 was necessary before any inactivation of test $I_{Ca}(P_2)$ could be demonstrated. The inactivation increased steadily to a maximum corresponding to the largest Ca^{2+} entry during the prepulse. For any calculated Ca^{2+} entry the I_{Ca}

inactivation was larger in the kindled than in the control granule cell (Fig. 8A). As expected, the Ca²⁺ entry during 100-ms prepulses was enlarged and induced further I_{Ca} inactivation in both control and kindled neurons. The Ca²⁺ entry calculated from I_{Ca} at steps more positive than +20 mV was gradually reduced in size and resulted in reduced inactivation of I_{Ca} (not shown). This finding provides further evidence for a close relationship between the influx of Ca²⁺ and the amount of I_{Ca} inactivation.

In both control and kindled neurons, BAPTA loading increased the amount of Ca²⁺ entering the cells (Fig. 8B) but only marginally affected I_{Ca} inactivation during P₂. Maximal Ca²⁺ entry elicited by 50- or 100-ms pulses was similar in control and kindled cells.

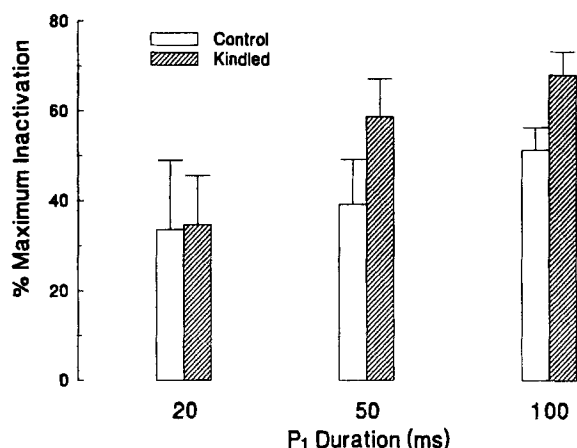


FIGURE 7. Extending the conditioning pulse duration (P₁ duration) in double-pulse experiments from 20, to 50, and to 100 ms to achieve increasing amounts of Ca²⁺ entry resulted in increased maximal inactivation of test Ca²⁺ currents. In all experiments, conditioning (20–100 ms) and test pulses (25 ms) were to +10 mV from a holding of –50 mV interrupted by a 50-ms repolarization to –50 mV. Recordings were performed in the absence of BAPTA. In control (*n* = 5) and

kindled (*n* = 7) granule cells, I_{Ca} were inactivated to about the same amount when 20-ms conditioning pulses were applied. Using a P₁ duration of 50 ms resulted in a significantly (*P* < 0.001, ANOVA) different I_{Ca} inactivation of control (*n* = 12) and kindled (*n* = 13) granule cells, which was still different when 100-ms P₁ durations were used (control, *n* = 3; kindled, *n* = 6).

Inactivation during Sustained Depolarization

In the absence of an exogenous Ca²⁺ chelator and during long (1 s) depolarizations, leak-unsubtracted I_{Ca} of comparable amplitudes showed an initial rapid decay from the peak, followed by a more gradual decay of the current. As shown for a control and a kindled granule cell (Fig. 9), the I_{Ca} decay was best approximated by a double-exponential expression with two time constants (τ_{fast} and τ_{slow}) of the form $y(t) = A \times \exp(-t/\tau_{fast}) + B \times \exp(-t/\tau_{slow}) + C$. The fast and slow components of inactivation were significantly different (*P* < 0.05, Mann-Whitney U-test) between control and kindled granule cells (Table II).

The effect of intraneuronal BAPTA on I_{Ca} inactivation during 1-s depolarizations is shown in Fig. 9 for a control and a kindled granule cell. The I_{Ca} decay was slowed down but could still be fitted by a double-exponential function. Both time constants (τ_{fast} and τ_{slow}) were significantly (*P* < 0.05, Mann-Whitney U-test) changed in the

presence of intracellular BAPTA in both control and kindled neurons and were no longer different from each other (Table II).

Recovery from Inactivation

Assuming an increased Ca^{2+} -dependent inactivation, the recovery from inactivation should also be slowed down in kindled neurons. To test this, the interpulse interval was gradually increased between conditioning prepulses (P_1 , 45 ms; to +10 mV) and test pulses (P_2 , 25 ms; to +10 mV). Both were evoked from a V_h of -50 mV. In Fig. 10

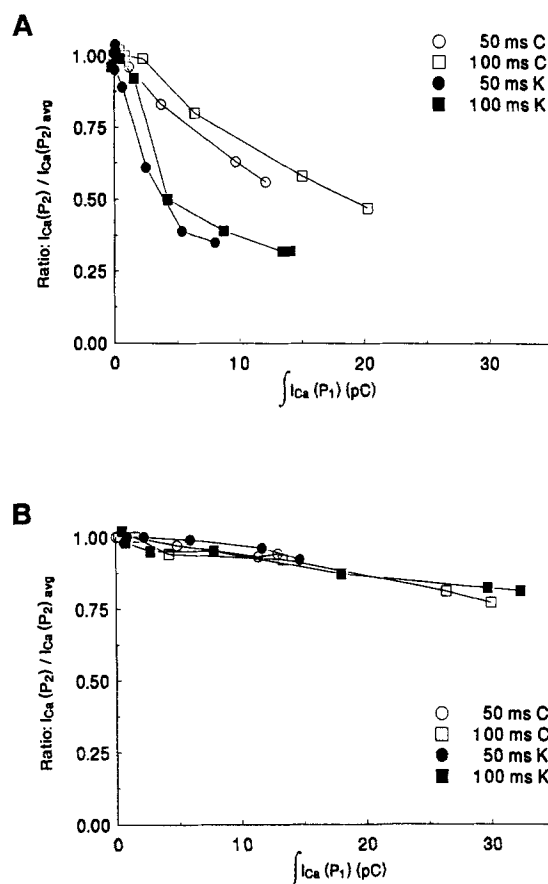


FIGURE 8. Inactivation of I_{Ca} as a function of Ca^{2+} entry in the absence (A) and presence of BAPTA (B). Double-pulse experiments with 50-ms and subsequent 100-ms conditioning pulses were performed for one control (50 ms C and 100 ms C) and one kindled granule cell (50 ms K and 100 ms K). The inactivation ratio $I_{Ca}(P_2)/I_{Ca}(P_2)_{avg}$ calculated as in Figs. 5 and 6 is plotted against Ca^{2+} entry during the conditioning pulse, measured by integrating the leak-corrected conditioning I_{Ca} . In the absence of BAPTA (A) the inactivation of Ca^{2+} currents is considerably larger in the kindled than in the control granule cell for each Ca^{2+} entry calculated. In the presence of BAPTA (B) the maximal Ca^{2+} entry is increased but the inactivation ratio is only marginally affected. Note that in each case (A and B) the decreasing inactivation ratio induced by I_{Ca} evoked from +20 to +80 mV is not plotted.

test I_{Ca} were elicited 50, 500, 1,000, and 2,000 ms after a conditioning I_{Ca} in a control (Fig. 10 A, upper panel) and kindled granule cell (Fig. 10 B, upper panel). Recovery from inactivation occurred faster in the control granule cell than in the kindled neuron.

The ratio between test $I_{Ca}(P_2)$ and the conditioning $I_{Ca}(P_1)$ is plotted as a function of increasing interstimulus intervals between 50 and 5,000 ms in the absence of BAPTA (open symbols). In control granule cells the test I_{Ca} started to recover immediately upon increasing interpulse intervals. In kindled granule cells recovery from inactivation started if the interstimulus interval was longer than 250 ms.

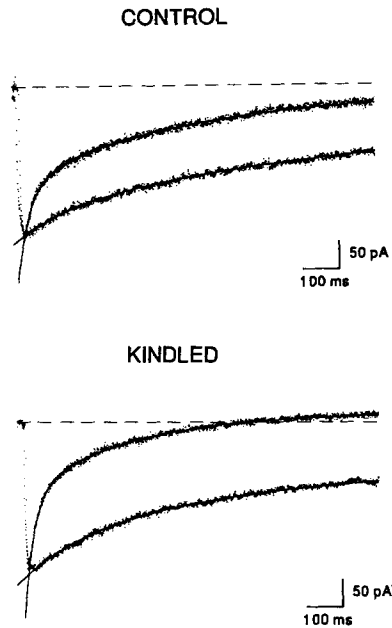


FIGURE 9. In the absence of BAPTA the raw (leak-unsubtracted) I_{Ca} decays faster in kindled than in control granule cells. After intracellular dialysis of 5 mM BAPTA/0.5 mM $CaCl_2$ the inactivation is slowed down and is about the same in both groups of neurons. Depolarizing pulses (1 s) from a V_h of -80 mV to $+10$ mV. For each trace, inactivation is best approximated by the following double-exponential expressions.

control (without BAPTA):

$$y(t) = -117.4 \times \exp(-t/33.5) - 154.5 \times \exp(-t/454.9) + 15.2$$

control (5 mM BAPTA/0.5 mM $CaCl_2$):

$$y(t) = -41.9 \times \exp(-t/131.5) - 160.0 \times \exp(-t/843.9) - 71.6$$

kindled (without BAPTA):

$$y(t) = -140.4 \times \exp(-t/26.3) - 139.5 \times \exp(-t/295.2) + 8.0$$

kindled (5 mM BAPTA/0.5 mM $CaCl_2$):

$$y(t) = -79.1 \times \exp(-t/196.3) - 123.9 \times \exp(-t/870.7) - 62.8$$

TABLE II

Comparison of the Two Decay Time Constants (τ_{fast} and τ_{slow}) of Ca^{2+} Currents during 1-s Depolarizing Pulses

	<i>n</i>	τ_{fast} (mean \pm SD)	τ_{slow} (mean \pm SD)
		<i>ms</i>	<i>ms</i>
Control	10	32.9 \pm 8.2 ^a	413.1 \pm 107.3 ^d
Kindled	6	25.3 \pm 4.6 ^b	293.4 \pm 85.7 ^c
Control + BAPTA	11	155.1 \pm 41.4 ^e	907.3 \pm 135.4 ^f
Kindled + BAPTA	6	169.2 \pm 44.3 ^e	969.4 \pm 160.5 ^f

The inactivation process was best fit by a double-exponential expression. The fast and slow time constants were significantly different between control and kindled granule cells only in the absence of BAPTA. Different superscript lowercase letters denote a significant difference ($P < 0.05$, Mann-Whitney U-test) between compared groups.

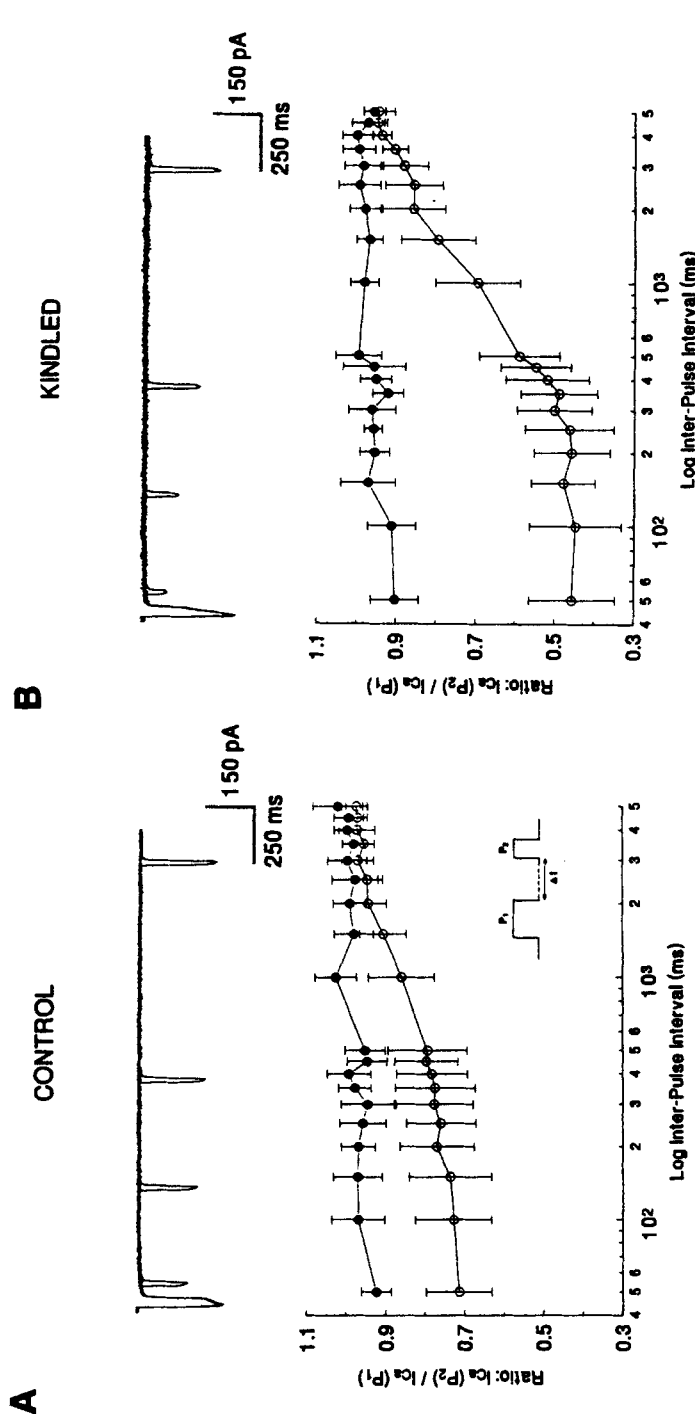


FIGURE 10. Recovery from inactivation is faster in a control (*A*) than in a kindled granule cell (*B*) in the absence of BAPTA. Superimposed raw current traces during 45-ms conditioning pulses, which were followed by test pulses (23 ms duration) after repolarizing potentials to -50 mV of various durations (50, 500, 1,000, and 2,000 ms). Both conditioning and test pulses are stepped to $+10$ mV. In the lower part of the figure, the ratio between normalized test Ca^{2+} currents $I_{Ca}(P_2)$ and normalized conditioning currents $I_{Ca}(P_1)$ is plotted as a function of interpulse intervals shown on a log scale. Note the different ratios of inactivation between control and kindled granule cells with short interpulse intervals and the delayed recovery from inactivation in the absence of BAPTA (\circ) in the kindled neuron. The fast recovery from inactivation in the presence of BAPTA (\bullet) is evident in both groups of neurons.

FIGURE 10. Recovery from inactivation is faster in a control (*A*) than in a kindled granule cell (*B*) in the absence of BAPTA. Superimposed raw current traces during 45-ms conditioning pulses, which were followed by test pulses (23 ms duration) after repolarizing potentials to -50 mV of various durations (50, 500, 1,000, and 2,000 ms). Both conditioning and test pulses are stepped to $+10$ mV. In the lower part of the figure, the ratio between normalized test Ca^{2+} currents $I_{Ca}(P_2)$ and normalized conditioning currents $I_{Ca}(P_1)$ is plotted as a function of interpulse intervals shown on a log scale. Note the different ratios of inactivation between control and kindled granule cells with short interpulse intervals and the delayed recovery from inactivation in the absence of BAPTA (\circ) in the kindled neuron. The fast recovery from inactivation in the presence of BAPTA (\bullet) is evident in both groups of neurons.

The recovery from inactivation was significantly enhanced in both groups of neurons after buffering intracellular Ca^{2+} by BAPTA addition (Fig. 10, filled symbols). Recovery from inactivation occurred gradually with increasing interpulse intervals in control ($n = 7$) and kindled ($n = 7$) granule cells.

Voltage Dependence of Inactivation

Recovery from inactivation was weakly voltage dependent ($\sim 5\%$ for 70 mV change in voltage) as tested by hyperpolarizing the membrane during the interpulse interval in the absence of BAPTA (Fig. 11). The conditioning pulse (P_1) to +10 mV achieved

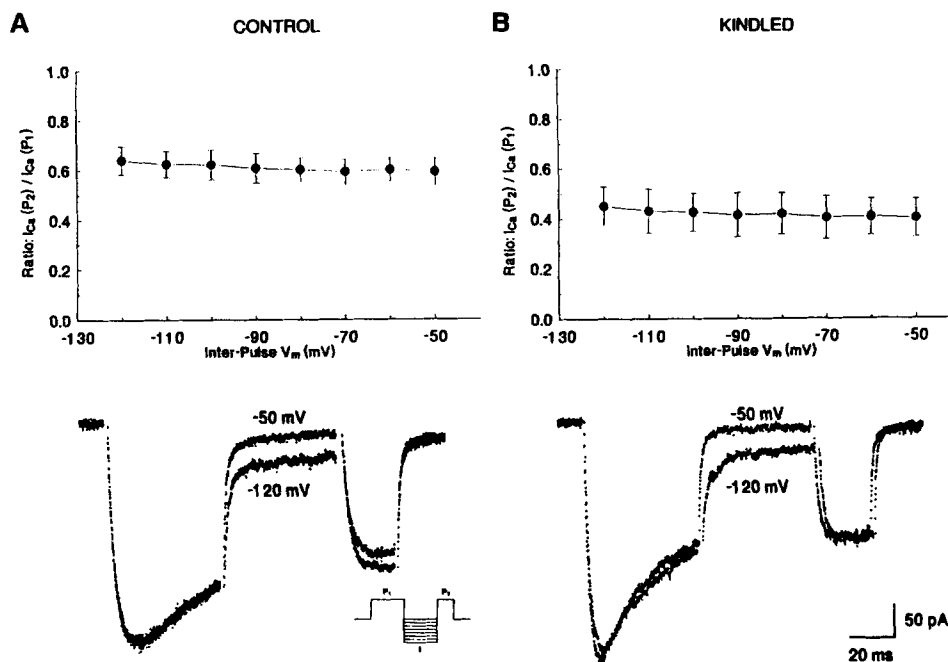


FIGURE 11. Voltage dependency accounts for $\sim 5\%$ of the recovery from inactivation over a range of 70 mV in control (*A*) and kindled (*B*) granule cells. The ratio between normalized test Ca^{2+} currents $I_{Ca}(P_2)$ and normalized conditioning currents $I_{Ca}(P_1)$ is plotted as a function of interpulse membrane potential V_m (-120 mV up to -50 mV) for nine control and seven kindled granule cells. Pulse protocol was as shown in the inset. P_1 (50 ms) was followed 50 ms later by P_2 (25 ms), both to +10 mV. Lower panels in *A* and *B* show superimposed traces of two raw (leak-unsubtracted) current recordings obtained with double pulses to +10 mV with different interpulse hyperpolarizations as indicated.

maximal inactivation of the test I_{Ca} (P_2 to +10 mV). When the interpulse voltage (50 ms) equalled the holding potential (-50 mV) maximal inactivation was $4.9 \pm 3.7\%$ ($n = 9$) in control and $5.0 \pm 2.3\%$ ($n = 7$) in kindled neurons, respectively, over that observed when the interpulse voltage was -120 mV (see superimposed current traces: control, Fig. 11 *A*; kindled, Fig. 11 *B*). This difference may be due to a slight

voltage-dependent reactivation of inactivated Ca^{2+} channels at potentials 70 mV hyperpolarized from rest.

Steady-State Inactivation

The steady-state inactivation of I_{Ca} was studied by varying the conditioning potential (1 s) and applying test pulses to +10 mV afterwards. Plots of normalized peak currents against conditioning potential are shown in Fig. 12. All inactivation curves

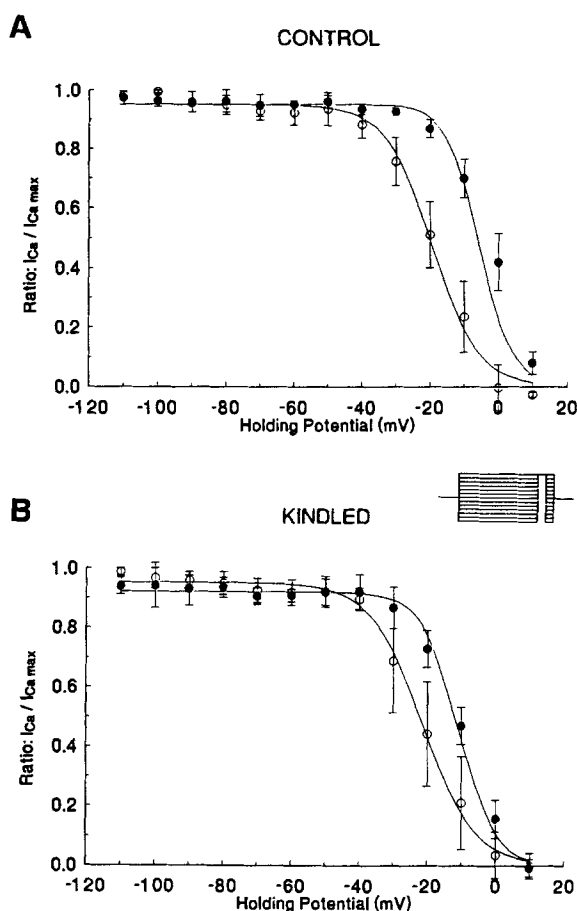


FIGURE 12. Steady-state inactivation of I_{Ca} in control (A) and kindled (B) granule cells in the absence (○) and presence of BAPTA (●) under the influence of different preceding conditioning holding potentials (1 s). Conditioning potentials started at -110 mV and were incremented by 10-mV steps while the command potential was kept constant at +10 mV. The ratio between evoked Ca^{2+} current at each conditioning potential and the maximal Ca^{2+} current evoked is plotted against the conditioning holding potential. In each case, the smooth curves are the best fits to the Boltzmann equation of the form: $I/I_{\text{max}} = \{1 + \exp[(V - V_{1/2})/k]\}^{-1}$. The curves were fit with the following values: $V_{1/2} = -19.41$, $k = 6.86$ (control, no BAPTA); $V_{1/2} = -5.71$, $k = 4.85$ (control, BAPTA); $V_{1/2} = -21.44$, $k = 7.65$ (kindled, no BAPTA); and $V_{1/2} = -10.99$, $k = 5.43$ (kindled, BAPTA).

are steeply voltage dependent. Fig. 12A illustrates the steady-state inactivation of I_{Ca} averaged from six control granule cells recorded without BAPTA (open symbols) and from five control cells recorded with intracellular BAPTA (filled symbols). The steady-state inactivation was well fitted by the following Boltzmann equation: $I/I_{\text{max}} = \{1 + \exp[(V - V_{1/2})/k]\}^{-1}$.

For control granule cells the best fit was obtained with a half-inactivating voltage ($V_{1/2}$) of -19.4 mV in the absence of BAPTA. In the presence of BAPTA the

inactivation curve was shifted to more positive potentials ($V_{1/2} = -5.7$ mV). The kindling process did not affect the steady-state inactivation characteristics of I_{Ca} as illustrated by inactivation curves recorded from kindled granule cells (Fig. 12 B). The $V_{1/2}$ was -21.4 mV ($n = 6$) in the absence of BAPTA and -11.0 mV ($n = 5$) with intraneuronal BAPTA present. These experiments also ruled out the contribution of a LVA I_{Ca} to the dominating HVA I_{Ca} .

DISCUSSION

We have described the activation and inactivation of HVA Ca^{2+} currents with or without exogenous intracellular Ca^{2+} chelators in dentate gyrus granule cells acutely dissociated from adult rats. The HVA Ca^{2+} channels display a mostly Ca^{2+} -dependent (current-dependent) inactivation when neurons are left to their endogenous Ca^{2+} buffering/sequestering mechanisms. We have also made use of a preparation in which a neuron-specific, high affinity cytosolic Ca^{2+} -binding protein, CaBP, is lost from the granule cells after kindling-induced epilepsy (Miller and Baimbridge, 1983; Baimbridge and Miller, 1984; Köhr et al., 1991). The changes in HVA Ca^{2+} current inactivation in kindled neurons are consistent with the hypothesis that this protein is a major constituent of the neuronal Ca^{2+} -sequestering machinery.

Whole-Cell Dialysis and Endogenous Ca^{2+} Buffering

The HVA Ca^{2+} current was the only substantial I_{Ca} in whole-cell, patch-clamp recordings from acutely dissociated control and kindled granule cells. We found no evidence of a LVA Ca^{2+} current, which is a prominent Ca^{2+} current in acutely dissociated neurons of the thalamus (Coulter, Huguenard, and Prince, 1989) or lateral geniculate nucleus (Hernández-Cruz and Pape, 1989). Our study is in agreement with previous work using whole-cell recordings in acutely dissociated hippocampal neurons and granule cells of enzyme-treated slices which solely possess HVA Ca^{2+} currents (Kay and Wong, 1987; Doerner, Pitler, and Alger, 1988; Fisher et al., 1990).

To assess the contribution of endogenous Ca^{2+} sequestering mechanisms to the inactivation of HVA Ca^{2+} currents, we have omitted any exogenous Ca^{2+} chelators from our recording solutions, an unusual approach in recordings from acutely dissociated neurons (Kay and Wong, 1987; Doerner et al., 1988; Coulter et al., 1989; Hernández-Cruz and Pape, 1989). Contrary to what would be expected in cells with an impaired intraneuronal Ca^{2+} homeostasis after acute enzymatic dissociation, the absence of an exogenous Ca^{2+} chelator was well tolerated by the acutely dissociated granule cells. Furthermore, in the presence of an intracellular high-energy phosphate support system (Forscher and Oxford, 1985), HVA Ca^{2+} currents remained remarkably stable and showed consistent activation/inactivation kinetics in whole-cell recordings lasting as long as 2 h, provided that sufficient time was allowed between eliciting two successive I_{Ca} . The I_{Ca} kinetics were indistinguishable from perforated patch recordings which do not perturb the cells' interior through dialysis (Horn and Marty, 1988). Therefore, the free Ca^{2+} contamination of our recording solutions appears to be negligible (less than or equal to the resting free Ca^{2+} in granule cells) as additionally demonstrated by the lack of discernible effects on HVA Ca^{2+} currents

and their inactivation characteristics when 5 μ M BAPTA was included in the recording pipette.

Activation and Inactivation of HVA Calcium Currents

As shown by Kay and Wong (1987) for acutely dissociated guinea pig hippocampal neurons, the activation/inactivation of HVA Ca^{2+} currents in rat dentate gyrus granule cells could be best described by m^2h type Hodgkin-Huxley kinetics. In the absence of exogenous Ca^{2+} chelators, the observed decrease in the inactivation rate at more depolarized potentials, where Ca^{2+} entry becomes progressively less, points to a Ca^{2+} dependence of the inactivation process. Furthermore, the significant increase in the inactivation rate in kindled neurons and the decrease in inactivation upon intracellular BAPTA loading indicate that the inactivation process is mostly dependent on intracellular Ca^{2+} accumulation. A small additional voltage-dependent (i.e., Ca^{2+} -independent) component of the inactivation process cannot be ruled out by our experiments.

It is less clear what mechanism, other than membrane voltage, influences the activation process of HVA Ca^{2+} channels. In the absence of exogenous Ca^{2+} chelators, the control activation rate of I_{Ca} was accelerated in kindled neurons, and this difference persisted after BAPTA loading. Thus, the faster activation rate of HVA Ca^{2+} currents in kindled neurons cannot be a consequence of an impaired intraneuronal Ca^{2+} buffering secondary to the loss of CaBP from these cells but may be a consequence of an enhanced CaM activity (see below).

With the endogenous intracellular Ca^{2+} -sequestering mechanisms intact, the time course of HVA Ca^{2+} current inactivation during long (1 s) depolarizing pulses could be best described by a fast and a slow exponential decay in both control and kindled granule cells. Both fast and slow time constants were shortened after kindling. This is in line with recordings in snail neurons (Gutnick et al., 1989) where the fast time constant was most affected by experimental alterations in the internal Ca^{2+} buffering, but the substantial amounts of EGTA used in those experiments may have obscured any changes in the slower decay time constant.

The differential Ca^{2+} -sensitive inactivation of HVA Ca^{2+} currents in control and kindled neurons is based on the assumption of an unaltered Ca^{2+} sensitivity of the inactivation process itself after kindling. Some findings in the present study may have resulted from a possible shift to the left in the Ca^{2+} sensitivity of the Ca^{2+} current inactivation mechanism. This alternative hypothesis, however, can be readily rejected. If the Ca^{2+} sensitivity of the inactivation process were enhanced in the kindled preparation, small but steady Ca^{2+} entries (like those evoked by holding the membrane potential slightly above the HVA Ca^{2+} current threshold) would be expected to inactivate Ca^{2+} currents more in kindled granule cells than in controls. However, no difference was found between the steady-state inactivation of control and kindled granule cells (cf. Fig. 12). It is, therefore, conceivable that most alterations in the inactivation of kindled HVA Ca^{2+} currents result from the impairment of intracellular Ca^{2+} sequestration.

The Role of CaBP to Limit a Rise in Intracellular Ca^{2+}

We have demonstrated that a change in Ca^{2+} current inactivation is correlated with a loss of intraneuronal CaBP in kindled neurons. The functional significance of this

correlation is only valid if CaBP did not diffuse out of the neurons during whole-cell recordings in control granule cells. This is unlikely for two reasons. First, the I_{Ca} inactivation kinetics recorded after the establishment of the whole-cell configuration showed no decrement over 30–40 min of recording. This may be regarded as evidence against a soluble protein being responsible for the control of inactivation. However, as judged from Table 1 of Pusch and Neher (1988), the experimentally measured diffusion rate of proteins in and out of patch pipettes does not appear to conform entirely to the linear relationship between diffusion rates and the 1/3 power of molecular weight which approximates the diffusion of other large organic molecules (Pusch and Neher, 1988). Thus no accurate predictions can be made about the rate of CaBP diffusion from the granule cells, particularly in conditions such as ours, where a substantial amount of large molecular weight protein was already present in the patch pipette. Second, even if a part of the soluble fraction may have diffused out of the cell, the membrane-bound fraction of CaBP, thought to be ~10% (Feher and Wasserman, 1978), may be sufficient to bind Ca^{2+} at the inner opening of HVA Ca^{2+} channels where the Ca^{2+} -dependent inactivation process resides (Yue et al., 1990).

We have also attempted to titrate the concentration of the exogenous Ca^{2+} chelator in a kindled neuron to mimic the Ca^{2+} -buffering properties of a control cell. These experiments turned out to be extremely difficult to interpret, probably because of the differences between CaBP and BAPTA with regard to Ca^{2+} -binding kinetics, intracellular pH, and Mg^{2+} sensitivities. For example, in double-pulse experiments (such as that illustrated in Fig. 5) the maximum inactivation in kindled neurons loaded with 1 mM BAPTA/0.1 mM $CaCl_2$ was 21.3% ($n = 3$). This inactivation fraction is different than that observed in kindled neurons loaded with 5 mM BAPTA/0.5 mM $CaCl_2$. Nevertheless, the inference regarding the endogenous Ca^{2+} buffering capacity of a control neuron remains inconclusive.

Perhaps the best test for the Ca^{2+} buffering capacity of CaBP in control granule cells would be to reintroduce purified CaBP into kindled neurons. This experiment may be hindered by the very slow diffusion of the 28-kD CaBP from the patch pipette into the cytosol, but further experiments with different Ca^{2+} binding proteins are underway to more accurately resolve the exact Ca^{2+} buffering capacity of control neurons.

Based on models of Ca^{2+} -dependent inactivation of HVA Ca^{2+} currents (Sherman, Keizer, and Rinzel, 1990), the role of CaBP could be to limit a maximal cytosolic Ca^{2+} rise at the cytoplasmic side of open channels. Otherwise, diffusion of Ca^{2+} to nearby closed channels may render them inactive. It is unlikely that binding of Ca^{2+} to CaBP could prevent the rapid inactivation of open Ca^{2+} channels that inactivate after binding of Ca^{2+} to a site nearby the inner mouth of the Ca^{2+} pore (Yue et al., 1990).

Change in Excitability after Kindling-induced Epilepsy

How then does the loss of intracellular CaBP translate into changes in excitability of kindled granule cells? Based on our findings, the electrophysiological consequences of the CaBP loss are twofold: (a) due to a more rapid activation of HVA Ca^{2+} currents in kindled neurons, more Ca^{2+} entry will stem from each low-frequency action potential fired by the granule cells (see Thayer and Miller, 1990); and (b) less Ca^{2+} entry will result during prolonged depolarizations of the granule cells or during

sustained high-frequency action potential firing. The latter alteration may be considered as a defence mechanism favoring the dampening of neuronal excitability. Thus, the loss of CaBP during kindling, together with the Ca^{2+} -dependent inactivation of I_{Ca} , may be regarded as a protective mechanism against excessive Ca^{2+} entry into neurons during prolonged epileptiform discharges.

However, other simultaneously activated cellular events secondary to the reduced capacity for intracellular Ca^{2+} buffering may easily tip the balance in favor of an enhanced excitation in kindled neurons. Some of these possibilities are presently under investigation. Based on similar affinities for Ca^{2+} between CaM and CaBP (Klee, Crouch, and Richman, 1980), it may be speculated that these two Ca^{2+} -binding proteins compete for the same Ca^{2+} entering the cell. With the loss of CaBP but preservation of CaM in kindled neurons (Miller and Baimbridge, 1983) more CaM may be activated which could lead to the enhanced activity of CaM-dependent neurotransmitter- or voltage-gated channels. It is noteworthy that the intraneuronal phosphatase calcineurin is a Ca^{2+} /CaM-dependent enzyme (Manalan, Krinks, and Klee, 1984). This phosphatase may in fact be responsible for temporarily cleaving off the phosphate from the phosphorylated active Ca^{2+} channels, rendering them inactive (Chad and Eckert, 1986). Naturally, CaM-dependent neuronal events may not be restricted to the control of Ca^{2+} channel inactivation. A persistently increased neuronal CaM activity may overstimulate the CaM-dependent protein kinase (CaM kinase II), resulting in its autophosphorylation and perhaps the loss of further Ca^{2+} requirement for its activity (Schulman, 1988). Finally, the demonstration of the Ca^{2+} buffering (or, more precisely, the Ca^{2+} rise-limiting) role of CaBP in the physiological range may shed some light on the selective Ca^{2+} -dependent vulnerability of neurons devoid of CaBP and related intracellular Ca^{2+} -binding proteins (McLachlan et al., 1987; Ichimiya et al., 1988; Seto-Ohshima et al., 1988; Scharfman and Schwartzkroin, 1989; Sloviter, 1989). Moreover, it may enable the future design of strategies aimed at the prevention and treatment of some Ca^{2+} -dependent neurodegenerative disorders.

We would like to thank J. T. Palmer for expert technical assistance. The comments of K. G. Baimbridge, J. R. Huguenard, H. Schulman, and R. W. Tsien were greatly appreciated. We are indebted to J. Dempster for providing the Strathclyde Electrophysiology Software.

This research was supported by NIH grants NS-12151 and NS-27528, and the Epilepsy Foundation of America. G. Köhr is a Deutsche Forschungsgemeinschaft Postdoctoral Fellow and I. Mody is a Klingenstein Fellow in the Neurosciences.

Original version received 8 March 1991 and accepted version received 6 June 1991.

REFERENCES

- Ashcroft, F. M., and P. R. Stanfield. 1981. Calcium dependence of the inactivation of calcium currents in skeletal muscle fibers of an insect. *Science*. 213:224–226.
- Baimbridge, K. G., and J. J. Miller. 1982. Immunohistochemical localization of calcium-binding protein in the cerebellum, hippocampal formation and olfactory bulb of the rat. *Brain Research*. 245:223–229.

- Baimbridge, K. G., and J. J. Miller. 1984. Hippocampal calcium-binding protein during commissural kindling-induced epileptogenesis: progressive decline and effects of anticonvulsants. *Brain Research*. 324:85–90.
- Brehm, P., R. Eckert, and D. Tillotson. 1980. Calcium-mediated inactivation of calcium current in *Paramecium*. *Journal of Physiology*. 306:193–203.
- Brown, A. M., K. Morimoto, Y. Tsuda, and D. L. Wilson. 1981. Calcium current-dependent and voltage-dependent inactivation of calcium channels in *Helix aspera*. *Journal of Physiology*. 320:193–218.
- Carafoli, E. 1987. Intracellular calcium homeostasis. *Annual Review of Biochemistry*. 56:395–433.
- Carbone, E., and H. D. Lux. 1984. A low-voltage activated fully inactivating calcium channel in vertebrate sensory neurons. *Nature*. 310:501–503.
- Celio, M. R. 1990. Calbindin-D_{28K} and parvalbumin in the rat nervous system. *Neuroscience*. 35:375–475.
- Chad, J. E., and R. Eckert. 1986. An enzymatic mechanism for calcium current inactivation in dialyzed *Helix* neurons. *Journal of Physiology*. 378:31–51.
- Coulter, D. A., J. R. Huguenard, and D. A. Prince. 1989. Calcium currents in rat thalamocortical relay neurons: kinetic properties of the transient, low-threshold current. *Journal of Physiology*. 414:587–604.
- Doerner, D., T. A. Pitler, and B. E. Alger. 1988. Protein kinase C activators block specific calcium and potassium current components in isolated hippocampal neurons. *Journal of Neuroscience*. 8:4069–4078.
- Eckert, R., and J. E. Chad. 1984. Inactivation of calcium channels. *Progress in Biophysics and Molecular Biology*. 44:215–267.
- Eckert, R., and D. Tillotson. 1981. Calcium-mediated inactivation of the calcium conductance in caesium-loaded giant neurones of *Aplysia californica*. *Journal of Physiology*. 314:265–280.
- Feher, J. J., and R. H. Wasserman. 1978. Evidence for a membrane-bound fraction of chick intestinal calcium-binding protein. *Biochimica et Biophysica Acta*. 540:134–143.
- Fenwick, E. M., A. Marty, and E. Neher. 1982. Sodium and calcium channels in bovine chromaffin cells. *Journal of Physiology*. 331:599–635.
- Fisher, R. E., R. Gray, and D. Johnston. 1990. Properties and distribution of single voltage-gated calcium channels in adult hippocampal neurons. *Journal of Neurophysiology*. 64:91–104.
- Forscher, P., and G. S. Oxford. 1985. Modulations of calcium channels by norepinephrine in internally dialyzed avian sensory neurons. *Journal of General Physiology*. 85:743–763.
- Fox, A. P., M. C. Nowycky, and R. W. Tsien. 1987. Kinetic and pharmacological properties distinguishing three types of calcium currents in chick sensory neurones. *Journal of Physiology*. 394:149–172.
- Gutnick, M. J., H. D. Lux, D. Swandulla, and H. Zucker. 1989. Voltage-dependent and calcium-dependent inactivation of calcium channel current in identified snail neurones. *Journal of Physiology*. 412:197–220.
- Hamill, O. P., A. Marty, E. Neher, B. Sakmann, and F. J. Sigworth. 1981. Improved patch-clamp techniques for high-resolution current recordings from cells and cell-free membrane patches. *Pflügers Archiv*. 391:85–100.
- Hernández-Cruz, A., and H.-C. Pape. 1989. Identification of two calcium currents in acutely dissociated neurons from the rat lateral geniculate nucleus. *Journal of Neurophysiology*. 61:1270–1283.
- Horn, R., and A. Marty. 1988. Muscarinic activation of ionic currents measured by a new whole-cell recording method. *Journal of General Physiology*. 92:145–159.

- Ichimiya, Y., P. C. Emson, C. Q. Mountjoy, D. E. Lawson, and C. W. Heizmann. 1988. Loss of calbindin-D_{28K} immunoreactive neurones from the cortex in Alzheimer-type dementia. *Brain Research*. 475:156–159.
- Kalman, D., P. H. O'Lague, C. Erxleben, and D. L. Armstrong. 1988. Calcium-dependent inactivation of dihydropyridine-sensitive calcium channels in GH₃ cells. *Journal of General Physiology*. 92:531–548.
- Kay, A. R., and R. K. S. Wong. 1987. Calcium current activation kinetics in isolated pyramidal neurones of the CA1 region of the mature guinea-pig hippocampus. *Journal of Physiology*. 392:603–616.
- Klee, C. B., T. H. Crouch, and P. G. Richman. 1980. Calmodulin. *Annual Review of Biochemistry*. 49:489–515.
- Köhr, G., C. E. Lambert, and I. Mody. 1990. Inactivation of HVA calcium currents in granule cells following kindling-induced epilepsy: the calcium buffering role of calbindin-D_{28K} (CaBP). *Society of Neuroscience Abstracts*. 16:622. (Abstr.)
- Köhr, G., C. E. Lambert, and I. Mody. 1991. Calbindin-D_{28K} (CaBP) levels and calcium currents in acutely isolated epileptic neurons. *Experimental Brain Research*. 85:543–551.
- Kostyuk, P. G., and O. A. Krishtal. 1977. Effects of calcium and calcium-chelating agents on the inward and outward current in the membrane of mollusc neurones. *Journal of Physiology*. 270:569–580.
- Manalan, A. S., M. H. Krinks, and C. B. Klee. 1984. Calcineurin: a member of a family of calmodulin-stimulated protein phosphatases. *Proceedings of the Society for Experimental Biology and Medicine*. 177:12–16.
- Marty, A., and E. Neher. 1983. Tight-seal whole-cell recording. In *Single-Channel Recording*. B. Sakmann and E. Neher, editors. Plenum Publishing Corp., New York, 107–122.
- Mattson, M. P., B. Rychlik, C. Chu, and S. Christakos. 1991. Evidence for calcium-reducing and excitoprotective roles for the calcium-binding protein calbindin-D_{28K} in cultured hippocampal neurons. *Neuron*. 6:41–51.
- McBurney, R. N., and I. R. Neering. 1987. Neuronal calcium homeostasis. *Trends in Neurosciences*. 10:164–169.
- McLachlan, D. R., L. Wong, C. Bergeron, and K. G. Baimbridge. 1987. Calmodulin and calbindin-D_{28K} in Alzheimer disease. *Alzheimer Disease and Associated Disorders*. 1:171–179.
- Miller, J. J., and K. G. Baimbridge. 1983. Biochemical and immunohistochemical correlates of kindling-induced epilepsy: role of calcium binding protein. *Brain Research*. 278:322–326.
- Mody, I., J. N. Reynolds, M. W. Salter, P. L. Carlen, and J. F. MacDonald. 1990. Kindling-induced epilepsy alters calcium currents in granule cells of rat hippocampal slices. *Brain Research*. 531:88–94.
- Mody, I., M. W. Salter, and J. F. MacDonald. 1989. Whole-cell voltage-clamp recordings in granule cells acutely isolated from hippocampal slices of adult or aged rats. *Neuroscience Letters*. 93:70–75.
- Morad, M., N. W. Davies, J. H. Kaplan, and H. D. Lux. 1988. Inactivation and block of calcium channels by photo-released Ca²⁺ in dorsal root ganglion neurons. *Science*. 241:842–844.
- Plant, T. D. 1988. Properties and calcium-dependent inactivation of calcium currents in cultured mouse pancreatic B-cells. *Journal of Physiology*. 404:731–747.
- Plant, T. D., N. B. Standen, and T. A. Ward. 1983. The effects of injection of calcium ions and calcium chelators on calcium channel inactivation in *Helix* neurons. *Journal of Physiology*. 334:189–212.
- Pusch, M., and E. Neher. 1988. Rates of diffusional exchange between small cells and a measuring patch pipette. *Pflügers Archiv*. 411:204–211.

- Racine, R. 1972. Modification of seizure activity by electrical stimulation. II. Motor seizure. *Electroencephalography and Clinical Neurophysiology*. 32:281–294.
- Scharfman, H. E., and P. A. Schwartzkroin. 1989. Protection of dentate hilar cells from prolonged stimulation by intracellular calcium chelation. *Science*. 246:257–260.
- Schroeder, J. E., P. S. Fischbach, M. Mamo, and E. W. McCleskey. 1990. Two components of high-threshold Ca²⁺ current inactivate by different mechanisms. *Neuron*. 5:445–452.
- Schulman, H. 1988. The multifunctional Ca²⁺/Calmodulin-dependent protein kinase. *Second Messenger and Phosphoprotein Research*. 22:39–112.
- Seto-Ohshima, A., D. E. Lawson, P. C. Emson, C. Q. Mountjoy, and L. H. Carrasco. 1988. Loss of matrix calcium binding protein containing neurons in Huntington's disease. *Lancet*. i:1252–1255.
- Sherman, A., J. Keizer, and J. Rinzel. 1990. Domain model for Ca²⁺-inactivation of Ca²⁺ channels at low channel density. *Biophysical Journal*. 58:985–995.
- Sloviter, R. S. 1989. Calcium-binding protein (calbindin-D_{28k}) and parvalbumin immunocytochemistry: localization in the rat hippocampus with specific reference to the selective vulnerability of hippocampal neurons to seizure activity. *Journal of Comparative Neurology*. 280:183–196.
- Thayer, S. A., and R. J. Miller. 1990. Regulation of the intracellular free calcium concentration in single rat dorsal root ganglion neurones in vitro. *Journal of Physiology*. 425:85–115.
- Tillotson, D. 1979. Inactivation of Ca conductance dependent on entry of Ca ions in molluscan neurons. *Proceedings of the National Academy of Sciences, USA*. 76:1497–1500.
- Swanson, G., editor. 1989. Special issue: calcium-effector mechanisms. *Trends in Neurosciences*. 12:417–478.
- Tsien, R. W. 1983. Calcium channels in excitable cell membranes. *Annual Review of Physiology*. 45:341–358.
- Tsien, R. Y. 1980. New calcium indicators and buffers with high selectivity against magnesium and protons. *Biochemistry*. 19:2396–2404.
- Yue, D. T., P. H. Backx, and J. P. Imredy. 1990. Calcium-sensitive inactivation in the gating of single calcium channels. *Science*. 250:1735–1738.
- Zar, J. R. 1984. *Biostatistical Analysis*. Prentice-Hall Inc., Englewood Cliffs, NJ. 1–718.